

Polystyrene Layers Grafted to Epoxy-Modified Silicon Surfaces

Igor Luzinov,[†] Daungrut Julthongpiput,[†] Hauke Malz,[‡] Jürgen Pionteck,[‡] and Vladimir V. Tsukruk^{*,†}*Department of Material Science & Engineering, Iowa State University, Ames, Iowa 50011, and Institute of Polymer Research Dresden, Hohe Strasse 6, D-01069 Dresden, Germany**Received June 9, 1999; Revised Manuscript Received November 4, 1999*

ABSTRACT: Carboxylic acid- and anhydride-terminated polystyrenes of different molecular weights from 4500 to 672 000 were grafted from melt onto silicon substrates modified with epoxysilane monolayer. The grafted chains are densely packed with a density close to the known value for the bulk material. The tethered polymer layers are very smooth, uniform, mechanically stable, and cover homogeneously the modified silicon. At the degree of polymerization (N) close to the critical molecular weight, the grafting process is the most effective, resulting in the grafted unperturbed macromolecules. We suggest that the grafting from the reactive polymer melt is controlled by steric constraints through the *minimum available free volume between the grafted macromolecules*, which is reachable by another reactive end. This volume correlates with the size of monomeric unit and varies very little with the molecular weight.

Introduction

Ultrathin end-grafted polymer layers can dramatically affect the surface properties of substrates such as adhesion,^{1,2} lubrication,³ wettability,^{4,5} friction,⁶ and biocompatibility.⁷ These layers have been the subject of intensive theoretical^{8–10} and experimental^{11–15} research. An important consideration in a great deal of these studies has been factors affecting the preparation of end-grafted polymer layers. The grafted layer can be built from polymers with particular end groups that react with the surface and are used as anchors. Such layers can be produced from either solution^{11,13} or melt.^{1,12,14–17} The irreversible adsorption from the melt offers potential advantages over grafting from solution mainly due to the screening of the excluded volume interactions.¹² Presumably, much more densely grafted layers can be formed from the melt than from solution. However, until now, there has been no clear answer on the question of how dense and thick polymer layers of different molecular weights can be fabricated from the melt by the “grafting to” technique.

Jones et al.¹² investigated the grafting of carboxyl and triethoxysilane-terminated polystyrene onto silicon wafers from the melt. The effect of the initial film thickness, annealing temperature, and time on the resulting grafted layers was investigated. It was found that the initial film thickness and the molecular weight of the polymer influence the layer morphology and thickness in a complicated way. However, for many of these polymer layers, a dewetting morphology was observed. Norton et al.¹ studied the dependence of the grafting density on the molecular weight of carboxylic acid-terminated polystyrene (PS–COOH) chains. The chain ends anchor from the melt to the epoxy thermoset surface through interaction between the carboxyl and epoxy groups. A linear decrease in the maximum achievable grafting density with molecular weight was observed. This was explained in part by an entropic barrier that opposes the addition of new chains to the

grafted layer. However, for the lowest molecular weight used (16 600), a deviation from this trend was observed.

The focus of the present study is the permanent grafting of a dense and homogeneous polymer layer from melt onto a modified silicon surface. We used carboxylic acid- and anhydride-terminated polystyrenes for the grafting from melt. The epoxysilane self-assembled monolayer (SAM) deposited on a silicon wafer was used as an anchoring surface. We previously showed that the epoxy-SAM is homogeneous with terminal epoxy groups mainly located at the SAM surface.¹⁸

Experimental Section

The epoxysilane compound (3-glycidoxypropyl)trimethoxysilane was purchased from Gelest, Inc. ACS-grade toluene and ethanol were obtained from Aldrich and were used as received. Highly polished single-crystal silicon wafers of {100} orientation (SAS, Inc.) were used as substrate. The substrates were first cleaned in an ultrasonic bath for 30 min, placed in a hot piranha solution (3:1 concentrated sulfuric acid/30% hydrogen peroxide) for 1 h, and then rinsed several times with high-purity water (18 M Ω cm, Nanopure). After being rinsed, the substrates were dried under a stream of dry nitrogen, immediately taken into the nitrogen-filled glovebox, and immersed in an epoxysilane solution (1 vol %) for 24 h. After the deposition was complete, the modified substrates were removed from solution and rinsed several times with toluene and ethanol. Detailed descriptions of the fabrication of epoxy-terminated SAMs and their interfacial properties can be found in our recent publications.¹⁸

The initial polymer film was spin-coated from 1 wt % toluene solution onto the wafers modified by the epoxysilane SAM. The thickness of these polystyrene films measured by ellipsometry was 40 ± 5 nm. The specimens were placed in a vacuum oven at 150 °C to enable the end groups to graft to the epoxy-terminated substrate. At high temperature, carboxylic groups are able to react with the epoxy groups of the monolayer.¹⁹ The mechanism of the reaction between the anhydride group and the epoxy group is also quite well understood.²⁰ It is caused by the reaction of impurities with the second component. Hydroxy impurities react with the anhydride of a dicarboxylic acid monoester. The resulting free carboxylic group reacts with an epoxy group of an ester, creating a new hydroxy group, which can react again with an anhydride. In this manner, the reaction continues. For carboxy-terminated PS, we expect to avoid the multiple anchoring due to the fact that all chains

* E-mail: vladimir@iastate.edu.

[†] Iowa State University.

[‡] Institute of Polymer Research Dresden.

are monofunctional. In addition, at given grafting conditions, PS monomeric units are incapable of reacting with SAMs.

We limited grafting time to 48 h because no significant changes were observed beyond first 18 h of grafting. In addition, significant increases of grafting time beyond several days at elevated temperature would increase chances for local thermal destruction. The unbounded polymer was removed by multiple washing with toluene, including washing in an ultrasonic bath. After eight washes, the thickness of the layer did not decrease with additional treatment in the ultrasonic bath. Sample fabrication was conducted under cleanroom 100 conditions.

Carboxy-terminated polystyrenes of different molecular weights from 4500 to 672 000 were obtained from Polymer Source, Inc. ($M_n = 45\,900$ and $672\,000$ g/mol) or Aldrich ($M_n = 143\,000$ g/mol) or were synthesized by "living" free radical polymerization ($M_n = 4500$, $16\,900$, and $28\,500$ g/mol). All samples possessed a relatively narrow molecular weight distribution with M_w/M_n in the range 1.05–1.4. Aliphatic acid-terminated PS ($M_n = 28\,500$ g/mol) has been prepared by the TEMPO method under conditions similar to those described by Baumert et al.²¹ 1.2 mol styrene were heated together with 3.3 mmol TEMPO and 3.3 mmol 4,4'-azo-bis(4-cyanopentanoic acid) to 130° C for 24 h. Camphersulfonic acid (0.1 g) was added to the system in order to accelerate the rate of polymerization and to reduce the autopolymerization reaction of styrene.²² To avoid unwanted side reaction during the sample preparation, the TEMPO group was removed by oxidation with *m*-chloroperbenzoic acid.²³ As an initiator for the atom transfer radical polymerization (ATRP), 4-(1-bromoethyl)benzoic acid resulting in benzoic acid-terminated PS ($M_n = 4500$ and $16\,900$ g/mol) has been used.²⁴ The polymerization was catalyzed by 2,2'-bipyridine and CuBr and was carried out at 130° C. Analogous to this, a phthalic anhydride-terminated PS was synthesized using 4-(bromomethyl)phthalic anhydride as an initiator ($M_n = 11\,900$ g/mol, $M_w/M_n = 1.42$).

Ellipsometry was performed with a COMPEL automatic ellipsometer (InOmTech, Inc.) at an angle of incidence of 70°. A three-layer model (silicon substrate + silicon oxide layer + polymer layer) was used to simulate experimental data and found thickness of polymer layer with refractive indices taken from literature (see for details Tsukruk et al.¹⁸). Original silicon wafers from the same batch and silicon wafers with SAM layer were tested independently and were used as reference samples for the analysis of grafted polymer layers.

Scanning probe microscopy (SPM) studies were performed on a Dimension 3000 (Digital Instruments, Inc.) microscope according to the known procedure.^{25,26} We used contact, friction, tapping, and phase modes to study morphology of these films in ambient air. Silicon nitride and silicon tips with spring constants from 0.2 N/m for contact mode to 50 N/m for tapping mode were used. Imaging was done at scan rates in the range 1–2 Hz, at normal loads ranging from several tens of newtons for contact mode to several newtons for tapping mode. For thickness evaluation from SPM data, we used a "scratch" test.²⁵ Scratches were produced by multiple scanning with a silicon nitride tip with a high normal load (several micronewtons). Testing of surface distribution of adhesive properties and elastic response was done in force volume mode.²⁶

To characterize the polymer layer, several parameters have been evaluated.²⁷ The surface coverage, Γ (mg/m²), was calculated from the ellipsometry and SPM thickness of the layer h (nm) by the following equation:

$$\Gamma = h\rho \quad (1)$$

where ρ (1.05 g/cm³) is the density of polystyrene.¹²

The grafting density, Σ (chain/nm²), i.e., the inverse of the average area per adsorbed chain, was determined by:

$$\Sigma = \Gamma N_A \times 10^{-21} / M_n = (6.023\Gamma \times 100) / M_n \quad (2)$$

where N_A is Avogadro's number and M_n (g/mol) is the number-average molecular weight of the grafted polymer.

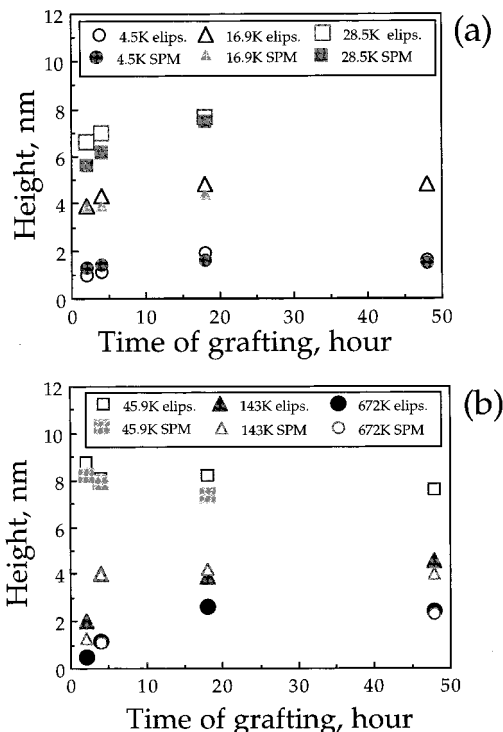


Figure 1. Layer height as measured by ellipsometry and SPM versus time of the grafting for the different molecular weights.

Finally, the distance between grafting sites, D , (nm) was calculated using the following equation:

$$D = (4/\pi\Sigma)^{1/2} \quad (3)$$

Results and Discussion

Figure 1 shows the kinetics of formation of the grafted layers for PS-COOH with different molecular weights from 4500 to 672 000. For all polymers studied, 18 h of grafting time is enough to approach a virtually constant thickness of a grafted layer. Only statistically insignificant differences were observed for samples with grafting times between 18 and 48 h. The layer heights obtained independently by ellipsometry and SPM are close to each other (within 5–10% error range, Figure 1). This indicates that the polymer is densely packed in the film with a refractive index (and density) very close to the known value for bulk material.

Figure 2 presents topographical images of the polymer layers at different deposition times for two selected molecular weights (low and high). Because the polymers are in a bad solvent (air) and are tethered to the surface, the chains are collapsed to a dense layer and do not dewet. For short deposition times, the low- and high-molecular-weight polymer layers display very different morphologies. The lower molecular weight polymers form densely packed nanometer-scale clusters distributed homogeneously and completely covering the substrate. When the layers are formed from high-molecular-weight polymer at short deposition times, the larger clusters are irregularly distributed on the surface, displaying the pattern of a partially dewetted film (Figure 2c). However, for all polymers, after 18–48 h of grafting time, the layer homogeneously covers the substrate and possesses very fine surface texture (Figure 2b,d).

Figure 3a shows the layer height and SPM roughness versus the degree of polymerization (N) for the polymer

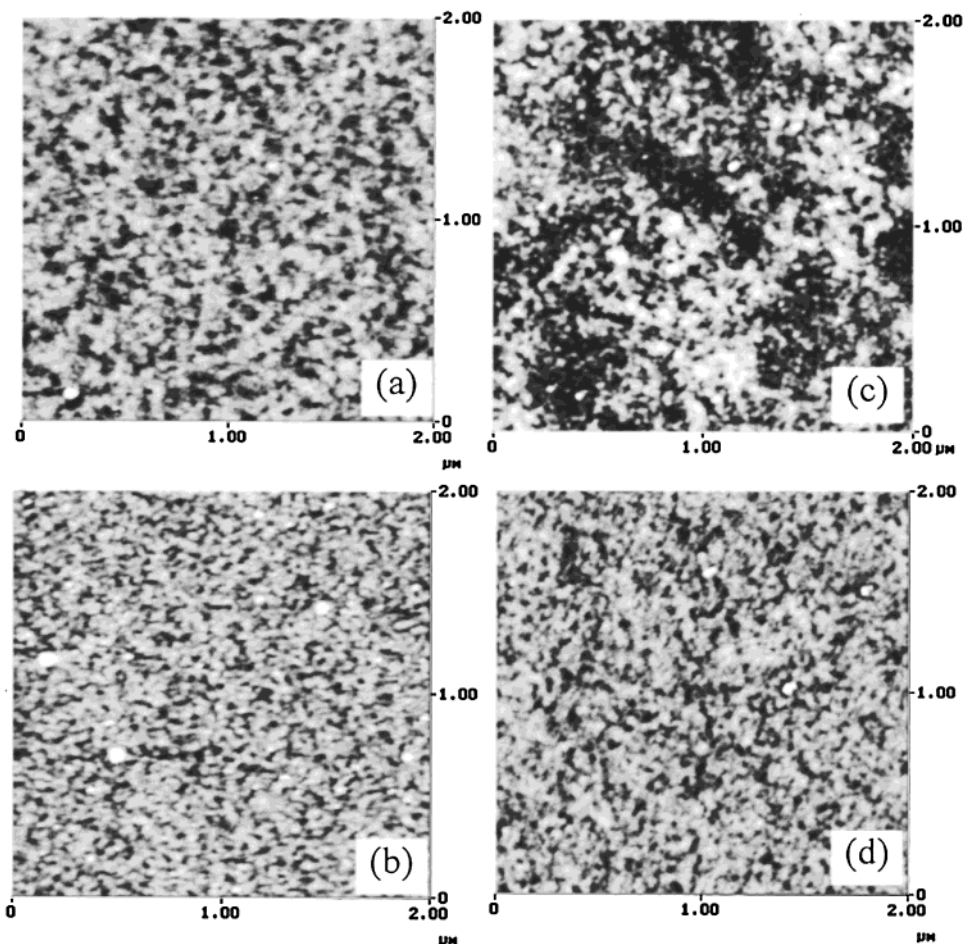


Figure 2. SPM topographical images of PS layers (a) and (c) after 2 and (b) and (d) 48 h of deposition for PS-COOH with (a) and (b) $M_n = 16\,900$ g/mol and (c) and (d) $M_n = 672\,000$ g/mol. The vertical scale is 10 nm.

layers at 18 h of deposition. Microroughness is 0.24 ± 0.06 nm within a $1 \times 1 \mu\text{m}^2$ area for all polymer layers after 18 h of deposition time. The microroughness is very close to the roughness of the supporting epoxysilane monolayer¹⁸ and much lower than that of the height of the layers. After 18 h of the deposition, the grafted layers practically reach a constant thickness and therefore represent the maximum possible grafting at the given conditions. These observations allow us to translate the film thickness into a surface coverage (Γ), grafting density (Σ), and distance between grafting sites (D) using eqs 1–3.

The layer height and surface coverage initially increase for the range $43 < N < 440$, passes through a maximum at $N = 440$, and then decreases (Figure 3a,b). The maximum is close to the critical entanglement molecular weight of PS, M_c , which is 31 200 g/mol ($N_c = 300$).²⁸ The same behavior is observed for the layer height scaled with $2R_g$ (Figure 3c), where R_g is the radius of gyration for the PS-COOH macromolecules, $R_g = a(N/6)^{1/2}$, where a is the statistical segment length ($a \approx 0.6$ nm for PS).^{29,30} The $h/2R_g$ ratio can be considered as a measure of chain stretching within the layer.¹¹ The grafted layers are somewhat squashed along the surface normal at all molecular weights except $M \sim M_c$ (Figure 3c). It reveals that at intermediate molecular weights close to M_c the polymer chains constituting the layer have the highest degree of the stretching, which is the unperturbed coil dimension. Figure 3c also shows how the distance between the grafting sites (D) reduced to $2R_g$ varies with the degree

of polymerization of the grafted polymer. The dependence shows a minimum at the intermediate molecular masses, which confirms the highest grafting density at $M_n \approx M_c$.

A significant decrease of grafting density is observed for two polymers with the highest molecular weights. This can be connected to a very low rate of the interfacial reaction for high-molecular-weight polymers due to slow diffusion of entangled chains. For such polymers, the reactive ends become kinetically trapped within the limited distance from the surface. Indeed, it was shown^{31–33} that for the polymer interfacial reaction, the effective reaction rate constant k is proportional to $1/(\ln N)$ and $1/N \ln N$ below and above M_c , respectively. Thus, the rate constants for entangled polymer decreases by several orders of magnitude at $M_n > M_c$, which prevents dense grafting within the time interval studied (<48 h).

The theory for polymer brushes predicts that the thickness of the end-grafted polymer layer h scales as $h \propto N\sigma$ in a poor solvent where $\sigma = (a/D)^2$ is the dimensionless grafting density.³⁴ Figure 4a shows that the prediction holds for the grafted polymer layers obtained in this work. For such systems, the grafting process as a first approximation can be considered as the sequential adsorption of disks with diameter $2R_g$ onto the surface. This approach predicts a linear dependence $D \propto N^{1/2}$ and, consequently, $\Sigma \propto 1/N$. The anticipated linear increase of the distance with the chain dimension is demonstrated in Figure 4b for various D/R_g ratios. However, as can be seen from the

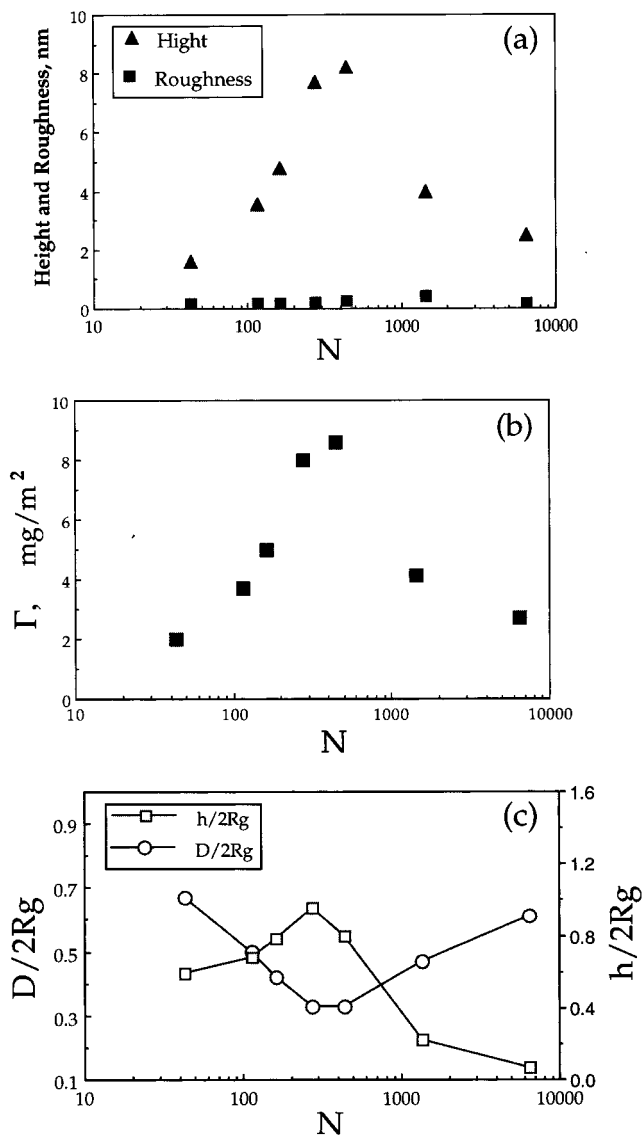


Figure 3. (a) Layer height and roughness, (b) surface coverage Γ (mg/m²), and (c) layer height and distance between grafting sites (D) reduced to $2R_g$ versus the degree of polymerization (N). Grafting time is 18 h.

Figure 4b, experimental data do not follow this relationship, and data points are scattered around the different lines. Consequently, the grafting density also does not follow $\Sigma \propto 1/N$ law.

It was proposed by Norton et al.¹ that Σ varies as $1-N$. This kind of behavior was confirmed for grafted PS layers on epoxy-terminated substrates.¹ We replotted these data in Figure 5a along with the linear approximation used in the comparison with our data. From this consideration, we excluded the highest molecular weight polymer due to the fact that it shows underestimated grafting density because of its nonequilibrium state. Obviously, a simple linear regression falls short of describing all experimental results, because it predicts the stopover of the grafting at the degree of polymerization close to 2000 (Figure 5a). However, in the experiment, the grafting was determined for these and higher molecular weights. As we observed, fitting of experimental data by nonlinear functions of the type $\Sigma \propto N^{-\delta}$ gives a more reasonable description of the experimental data that shows a minute variation of grafting density for high molecular weight. The param-

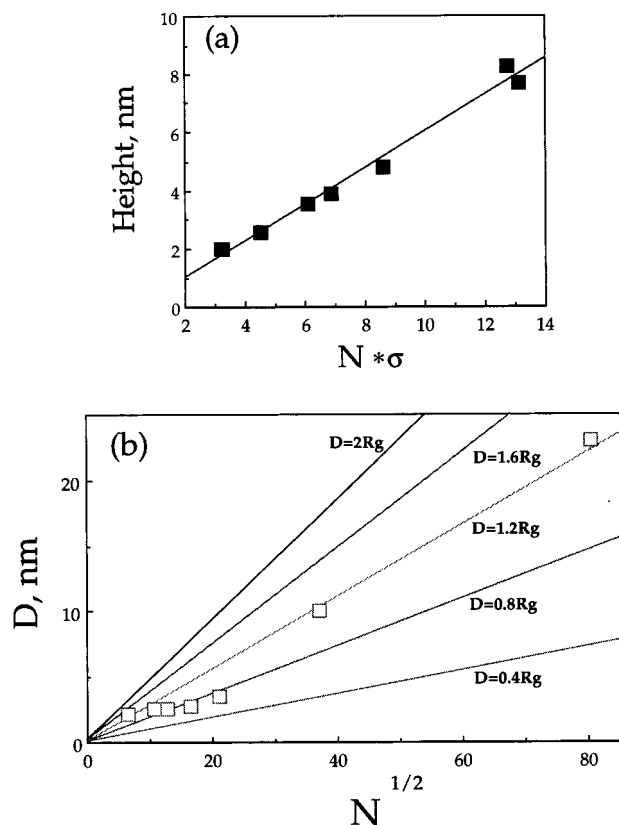


Figure 4. Plots of (a) grafted layer height versus $N \cdot \sigma$ and (b) distance between grafting sites (D) versus $N^{1/2}$.

eter δ is in the range 0.4–0.6 for data combined from our experiments and those of Norton et al.¹ (Figure 5a).

Here, we discuss a simple geometrical model that adequately describes observed experimental behavior (Figure 6). Of course, the model discussed below is too simplistic to provide comprehensive representation of our system but, nevertheless, provides a valuable insight in possible nature of steric constraints during the grafting process. A major assumption of this model is that steric constraints between two grafted chains prevent grafting of an additional chain end, which reaches the surface at a later time. In the course of the grafting, the distance between the anchored chains decreases to the level that the segments with the restricted mobility overlap. The mobility of these segments is limited, because they or their neighbors are chemically connected to the surface. At such a critical distance, the surface became screened and there is no enough free volume in vicinity of interface for another segment to access a binding site. We suggest that the limiting free volume can be characterized by the distance between the surface and the intersection point of neighboring overlapped grafted macromolecules, d , in their unperturbed state (Figure 6). Indeed, chains adopt random coil conformation during the grafting process from melt despite the fact that they are "squashed" in their final "dry" state.

In the framework of this geometrical model, an increase of the degree of overlapping (decrease of D) effectively leads to an increased "screening" of the surrounding surface. From geometrical consideration, one can obtain the relationship:

$$D^2 = 4d(2R_g) - 4d^2 \quad (4)$$

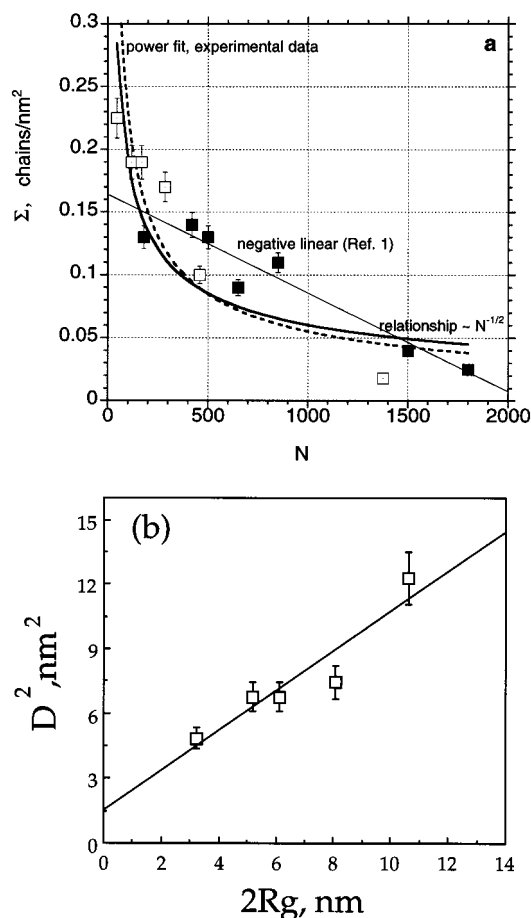


Figure 5. Plots of (a) grafting density Σ (chain/nm²) versus N and (b) distance between grafting sites (D) versus chain dimension. Grafting time was 18 h for our experimental data. Filled squares are data from Norton et al.,¹ and the linear fit is done for data points from Norton et al.¹ Power fit includes all data points from both this study and that of Norton et al.¹

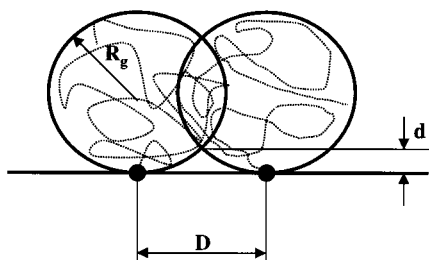


Figure 6. Schematic representation of two neighboring grafted chains and definition of the limiting distance d .

which is valid for $R_g > 2d$. Thus, for this model,

$$D \propto R_g^{1/2} \text{ and } D \propto N^{1/4} \quad (5)$$

with a slope equal to $4d$.

By plotting D^2 versus $2R_g$, we can estimate the critical distance d . For the evaluation, we included only data for the polymers with molecular weight close to and lower than M_C , because they certainly approach equilibrium grafting. The D^2 versus $2R_g$ dependence indeed shows a virtually linear relationship (Figure 5b). The slope of a linear fit corresponds to $d = 0.23$ nm, which is close to the length of the PS monomeric unit (0.25 nm). This dimension is reasonably close to the suggested meaning of the parameter d as the low limiting size of the polymer chain, which can be placed onto the surface

between two previously grafted chains (Figure 6). From the eq 5, simple arguments lead to a scaling law:

$$\Sigma \propto N^{-1/2} \quad (6)$$

In fact, experimental data obtained here and those from Norton et al.¹ lie between two limiting cases: a linear decrease as discussed in Norton et al.¹ and the $N^{-1/2}$ relationship (eq 6) derived here from steric arguments. However, eq 6 follows the experimental behavior at high molecular weights. It is interesting to notice that the same scaling prediction was found for the polymer-polymer coupling reaction at the polymer/polymer interface.^{31,32} It was pointed that the effective reaction rate constant becomes negligibly small when the area per chain drops below $N^{1/2}$.

Finally, we tested the lateral distribution of surface properties of grafted PS layers. We observed that the shear response of PS layers is extremely homogeneous, as revealed by friction force microscopy (see Tsukruk et al.¹⁸). Then, we tested the distribution of adhesive forces and elastic response of PS layer by doing force volume testing (Figure 7). This technique allows pixel-by-pixel probing of surface properties by collection of force-distance curves over selected surface area.²⁵ We selected an area around the intentionally damaged area (hole) produced by the SPM tip to emphasize the properties of the surrounding untouched polymer layer. We collected the data in a 32×32 array and extracted adhesive force values (pull-off forces as defined by the force-distance curve²⁶) and elastic compression moduli. Data processing was done according to our previously published work.³⁵ As can be seen from topographical data (top of Figure 7), the worn area within PS layer is surrounded by polymer debris accumulated during "digging" procedure. Elastic moduli and adhesive forces are much lower along the debris area, but they are very homogeneous on the PS layer surface far from the damaged area. From the analysis of elastic modulus depth profiles according to Chizhik et al.,³⁵ we concluded that the SPM tip indents and compresses very thin polymer layers and probes the underlying solid substrate. However, after tip retraction, the initial surface morphology (thickness, roughness, homogeneity) is completely restored without any trace of high local compression. This behavior indicates that the tethered polymer layer can sustain very high local mechanical distortions without compromising its integrity. It worth noting that physically adsorbed PS layers are completely destroyed under comparable probing conditions.¹⁸

In conclusion, we fabricated *dense and homogeneous PS polymer layers permanently grafted* to the epoxy-modified surface of silicon wafers. These layers did not dewet from the modified silicon surface and did not desorb in a good solvent under ultrasonic treatment. We proposed that the grafting from the melt is controlled by steric constraints through the limiting free volume between the grafted macromolecules that can be accessed by the late-arriving polymer chain. The reactive SAM surface becomes inaccessible for the reactive chain ends if the characteristic dimension d becomes less than the size of a monomeric unit. At high molecular weight, the grafting density is limited by the very low rate of the interfacial diffusion. Grafted polymer layers obtained here possess laterally homogeneous morphology and very evenly distributed adhesive, shear, and elastic properties. They are very firmly tethered to the surface

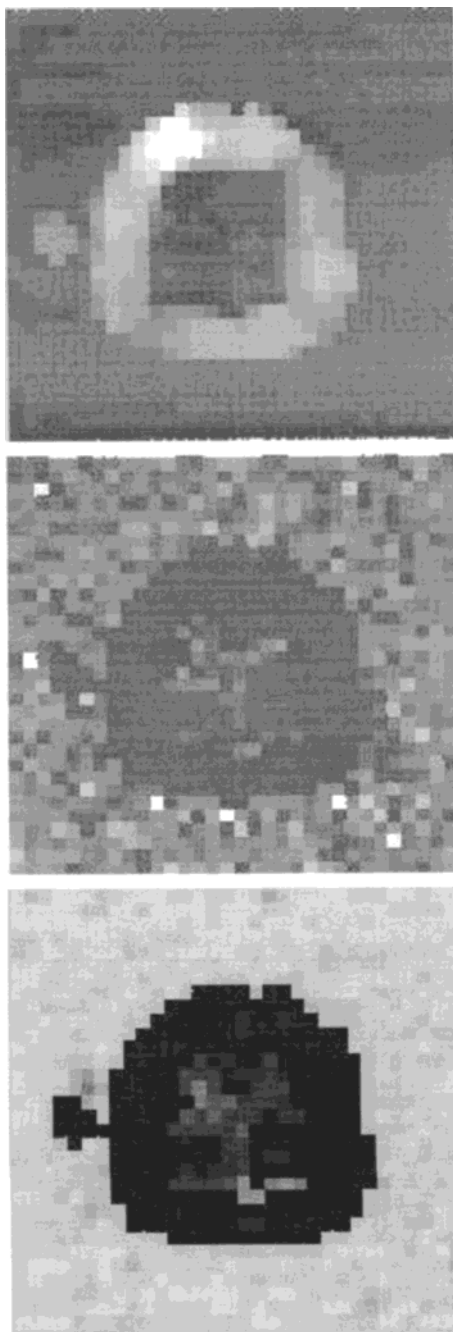


Figure 7. Topography (top, Z range is 40 nm), elasticity (middle, Z range is 100 GPa), and adhesion (bottom, Z range is 950 nN) for PS layer of 8 nm thick with the worn area in the center. Collected for 32×32 pixels, lateral size is $3 \times 3 \mu\text{m}$.

and can sustain significant shear stresses that far exceed those needed to damage physically absorbed polymer films.

Acknowledgment. This work is supported by The National Science Foundation, Grant CMS-9610408 and Contract AFOSR F49620-93-C-0063. The authors thank Dr. S. Minko and Dr. V. Gorbunov for helpful discussion and Z. Huang for technical help in obtaining Figure 7.

References and Notes

- (1) Norton, L. J.; Smiglova, V.; Pralle, M. U.; Hubenko, A.; Dai, K. H.; Kramer, E. J.; Hahn, S.; Beglund, C.; DeKoven, B. *Macromolecules* **1995**, *28*, 1999.
- (2) Lee, L. H. *Adhesion and Adsorption of Polymers*; Plenum Press: New York, 1980.
- (3) Inoue, H.; Uyama, Y.; Uchida, E.; Ikada, Y. *Cell Mater.* **1992**, *2*, 21.
- (4) Luzinov, I.; Minko, S.; Senkovsky, V.; Voronov, A.; Hild, S.; Marti, O.; Wilke, W. *Macromolecules* **1998**, *31*, 3945–3952.
- (5) Ruckert, D.; Gueskens, G. *Eur. Polym. J.* **1996**, *32*, 201.
- (6) Tomita, N.; Tamai, S.; Okajima, E.; Hirao, Y.; Ikeuch, K.; Ikada, Y. *J. Appl. Biomater.* **1994**, *5*, 175.
- (7) Ruckenstein, E.; Chang, D. B. *J. Colloid Interface Sci.* **1988**, *123*, 170.
- (8) De Gennes, G. *Macromolecules* **1980**, *13*, 1069.
- (9) Milner, S.; Witten, T.; Cates, M. *Macromolecules* **1988**, *21*, 2610.
- (10) Solis, F. J.; Tang, H. *Macromolecules* **1996**, *29*, 7953.
- (11) Karim, A.; Tsukruk, V. V.; Douglas, J. F.; Satija, S. K.; Fetters, L. J.; Reneker, D. H.; Foster, M. D. *J. Phys. II France* **1995**, *5*, 1441.
- (12) Jones, R. A. L.; Lehnert, R. J.; Schonerr, H.; Vancso, J. *Polymer* **1999**, *40*, 525.
- (13) Auroy, P.; Auvray, L.; Leger, L. *Macromolecules* **1991**, *24*, 5158.
- (14) Clarke, C. J.; Jones, R. A. L.; Clough, A. S. *Polymer* **1996**, *37*, 3813.
- (15) Clarke, C. J. *Polymer* **1996**, *37*, 4747.
- (16) Cosgrove, T.; Turner, M. J.; Thomas, D. R. *Polymer* **1997**, *38*, 3885.
- (17) Clarke, C. J.; Jones, R. A. L.; Edwards, J. L.; Clough, A. S.; Penfold, J. *Polymer* **1994**, *35*, 4065.
- (18) Tsukruk, V. V.; Luzinov, I.; Julthongpiput, D. *Langmuir* **1999**, *15*, 3029. Luzinov, I.; Julthongpiput, D.; Liebmann-Vinson, A.; Cregger, T.; Foster, M. D.; Tsukruk, V. V. *Langmuir*, accepted for publication.
- (19) Koning, C.; Van Duin, M.; Pagnouille, C.; Jerome, R. *Prog. Polym. Sci.* **1998**, *23*, 707.
- (20) Fisch, W.; Hofman, W. *Makromol. Chem.* **1961**, *44*, 8.
- (21) Baumert, M.; Muelhaupt, R. *Macromol. Rapid. Commun.* **1997**, *18*, 787.
- (22) Georges, M. K.; Veregin, R. P. N.; Katzmaier, P. M.; Hamer, G. K.; Saban, M. *Macromolecules* **1994**, *27*, 7228.
- (23) Malz, H.; Komber, H.; Voigt, D.; Pionteck, J. *Macromol. Chem. Phys.* **1998**, *199*, 583.
- (24) Malz, H.; Komber, H.; Voigt, D.; Hopfe, I.; Pionteck, J. *Macromol. Chem. Phys.* **1999**, *200* (3), 642.
- (25) Tsukruk, V. V. *Rubber Chem. Technol.* **1997**, *70* (3), 430.
- (26) Tsukruk, V. V.; Reneker, D. H. *Polymer* **1995**, *36*, 1791.
- (27) Ratner, B.; Tsukruk, V. V., Eds. *Scanning Probe Microscopy in Polymers*, ACS Symp. Ser. **1998**, 694.
- (28) Henn, G.; Bucknall, D. G.; Stamm, M.; Vanhoorne, P.; Jerome, R. *Macromolecules* **1996**, *29*, 4305.
- (29) Wool, R. P. *Polymer Interfaces: Structure and Strength*; Hanser/Gardner Pub.: Cincinnati, OH, 1995.
- (30) Sperling, L. H. *Introduction to Physical Polymer Science*; John Wiley & Sons: New York, 1992.
- (31) Siqueira, D. F.; Kohler, K.; Stamm, M. *Langmuir* **1995**, *11*, 3092.
- (32) O'Shaghnessy, B.; Sawhney, U. *Phys. Rev. Lett.* **1996**, *76*, 3444.
- (33) O'Shaghnessy, B.; Sawhney, U. *Macromolecules* **1996**, *29*, 7230.
- (34) Fredrickson, G. H. *Phys. Rev. Lett.* **1996**, *76*, 3440.
- (35) Auroy, P.; Auvray, L.; Leger, L. *Phys. Rev. Lett.* **1991**, *66*, 719.
- (36) Chizhik, S. A.; Huang, Z.; Gorbunov, V. V.; Myshkin, N. K.; Tsukruk, V. V. *Langmuir* **1998**, *14*, 2606. Tsukruk, V. V.; Huang, Z.; Chizhik, S. A.; Gorbunov, V. V. *J. Mater. Sci.* **1998**, *33*, 4905. Tsukruk, V. V.; Huang, Z. *Polymer* **1999**, accepted for publication.

MA990926V